Electronic Supplementary Material (ESI) for Journal of Materials Chemistry A.

Positively charged membranes with fine-tuned nanopores for ultrafast and high-precision cation separation

Min Gyu Shin[a‡], Jin Young Seo[a‡], Hosik Park[b], You-In Park[b], Seulgi Ji[c], Sun Sook Lee[c], Jung-Hyun Lee[a*]

a Department of Chemical and Biological Engineering, Korea University, 145 Anam-ro, Seongbuk-gu, Seoul 02841, Republic of Korea. E-mail: leejhyyy@korea.ac.kr.
b Green Carbon Research Center, Chemical and Process Technology Division, Korea Research Institute of Chemical Technology, Daejeon, 34114, Republic of Korea
c Thin Film Materials Research Center, Korea Research Institute of Chemical Technology, Daejeon 34114, Republic of Korea

SUPPLEMENTARY INFORMATION

S1. Synthesis and characterization of PSQA.

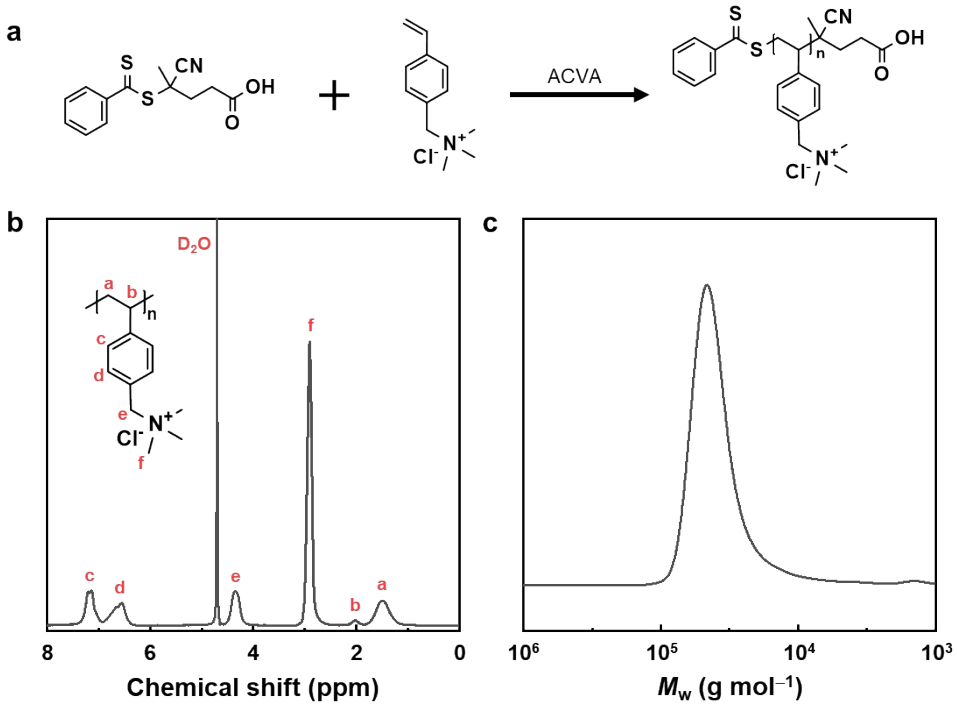

d

Conversion (%)	Absolute molecular weight (kg mol^{-1})	Relative molecular weight (kg mol^{-1})		
		M_w	M_n	M_w/M_n
98.9	54.6	56.0	45.0	1.2

Fig. S1. (a) Synthesis procedure, (b) ^{1}H nuclear magnetic resonance (^{1}H NMR, Avance III^{TM} HD 400 MHz NMR spectrometer, Bruker) spectra, (c) gel permeation chromatography (GPC, 2695 Separation Modules, Waters) spectra, and (d) corresponding molecular weights of PSQA. Polymerization conversion and absolute molecular weight were obtained from ^{1}H NMR. The weight- (M_w) and number-averaged (M_n) molecular weights and polydispersity index (M_w/M_n) were obtained from GPC analysis using H_2O as an eluent.

S2. Physicochemical properties of PSQA.

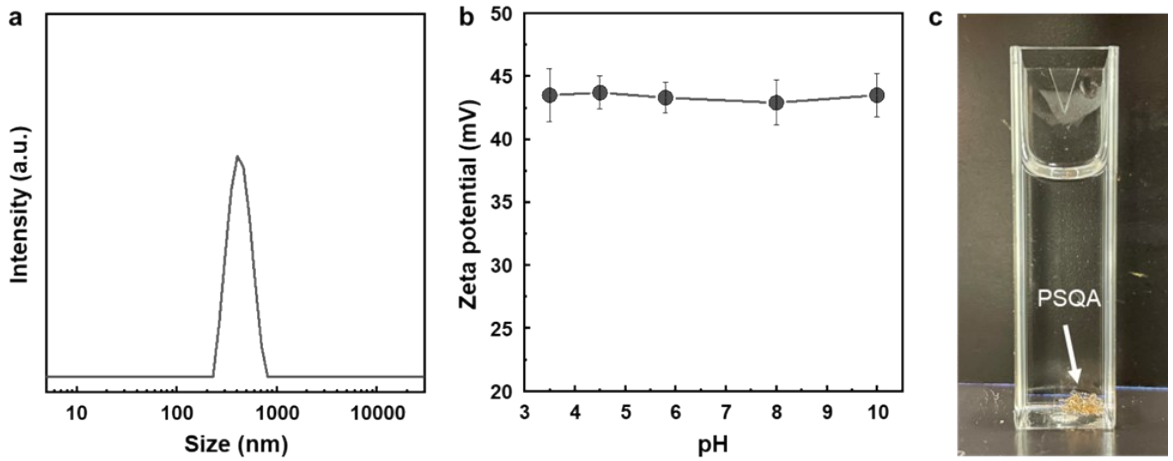

Fig. S2. (a) Hydrodynamic size (measured by dynamic light scattering (DLS, ELSZ-2000, Otsuka Electronics) with an aqueous solution of 0.3 mM PSQA), (b) zeta potential, and (c) solubility in DMSO of PSQA (PSQA rapidly precipitates in DMSO due to its poor solubility in DMSO).

S3. Optimization of the process parameters of the SD technique.

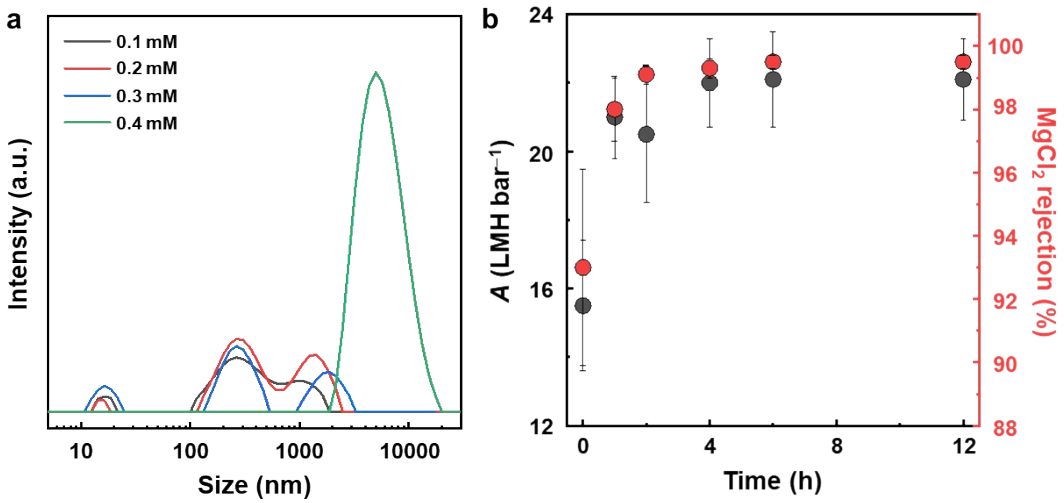

Fig. S3. (a) Hydrodynamic size (measured by DLS) of PSQA in the DMSO/water mixture (ϕ_{DMSO} = 0.95) as a function of PSQA concentrations. The PSQA concentration higher than 0.3 mM led to the significant increase in the hydrodynamic size of PSQA due to its severe self-aggregation. (b) Water permeance (A) and $MgCl_2$ rejection of the PENF-SD membrane prepared with the DMSO/water mixture (ϕ_{DMSO} = 0.95) containing 0.3 mM PSQA as a function of the activation time.

S4. XPS data of the prepared membranes.

a

Membrane	XPS Atomic composition (%)			O/N ratio
	C	N	O	
PERO	71.7	16.8	11.5	1.46
PENF	73.3	11.7	15.0	1.28

b

Membrane	Deconvoluted N1s peaks (etching time = 0 s)	Percentage (%)	
		Before acid/base cleaning	After acid/base cleaning
PENF-Dip	N1 (O=C–N)	68.3	55.9
	N2 ($R–NH_2$)	20.5	37.0
	N3 ($R–N^+R_3$)	11.2	7.1
PENF-SD	N1 (O=C–N)	58.5	56.4
	N2 ($R–NH_2$)	16.6	19.4
	N3 ($R–N^+R_3$)	24.9	24.2

c

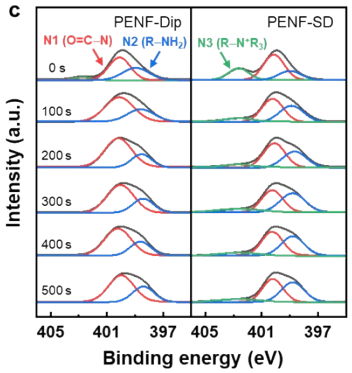

Fig. S4. (a) XPS atomic compositions of the PERO and PENF membranes. (b) Area percentage of the deconvoluted XPS N1s peaks (etching time = 0 s) of the PENF-Dip and PENF-SD membranes before and after acid/base cleaning. (c) XPS depth profiles (with respect to the etching time from 0 to 500 s) of the deconvoluted N1s peaks of the PENF-Dip and PENF-SD membranes after acid/base cleaning.

S5. Structure of the prepared membranes after acid/base cleaning.

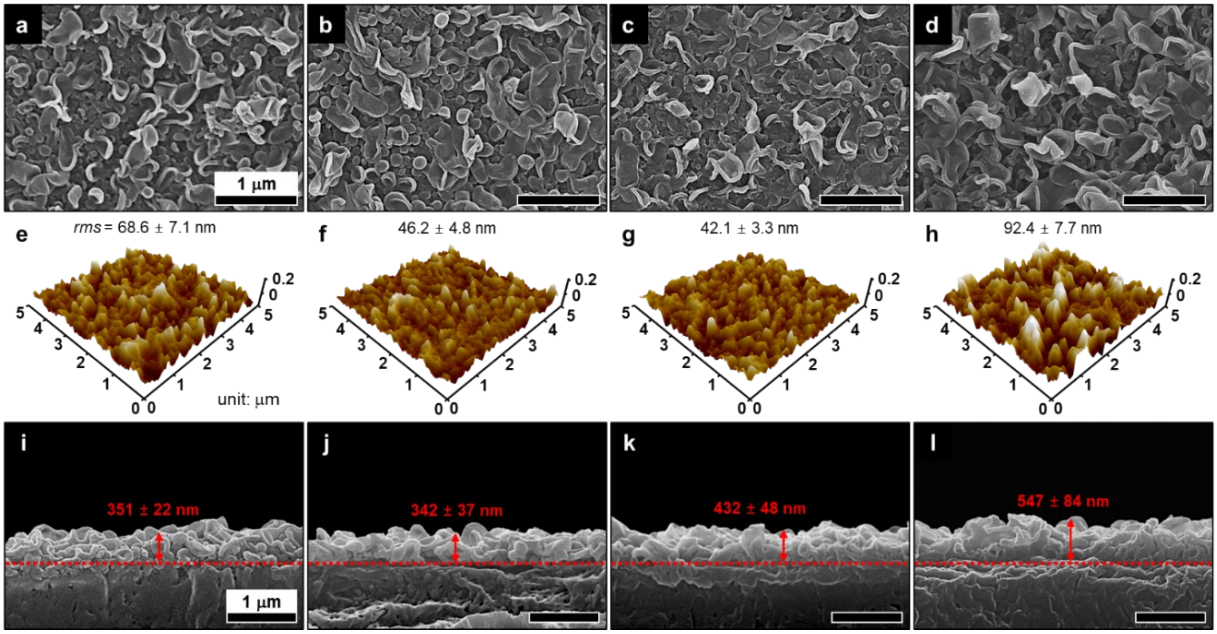

Fig. S5. (a–d) SEM surface, (e–h) AFM topological surface (including rms surface roughness), and (i–l) SEM cross-sectional images of the PERO (a, e, i), PENF (b, f, j), PENF-Dip (c, g, k), and PENF-SD (d, h, l) membranes after acid/base cleaning. The error bars represent the standard deviation of three replicate experiments.

S6. Pore structure and surface charge of the membranes.

a

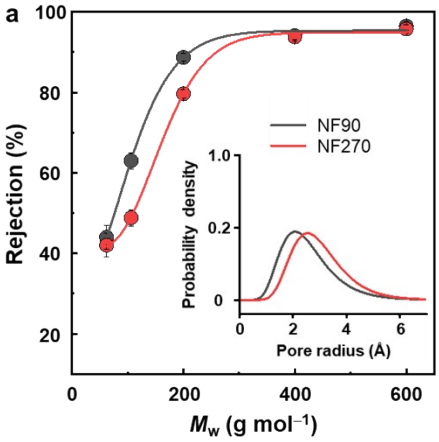

b

Membrane	MWCO (g mol^{-1})	Mean pore size (Å)	Geometric standard deviation	Surface zeta potential (mV)
PERO	112.2	2.2	1.26	−20.8 ± 1.3
PENF	220.4	2.6	1.42	−10.9 ± 1.5
PENF-Dip	222.5	2.7	1.48	27.8 ± 0.9
PENF-SD	280.7	3.2	1.34	32.1 ± 0.5
NF90	211.8	2.4	1.57	-25.5 ± 1.1
NF270	259.7	2.8	1.47	-40.1 ± 2.1

Fig. S6. (a) Rejection for neutral organic solutes with different molecular weights (M_w) and (inset) corresponding pore size distribution profiles of commercial NF (NF90 and NF270) membranes. (b) Pore structure (MWCO, mean pore size, and geometric pore size standard deviation) and surface zeta potential of the prepared and commercial membranes.

S7. Compaction behavior of the prepared membranes.

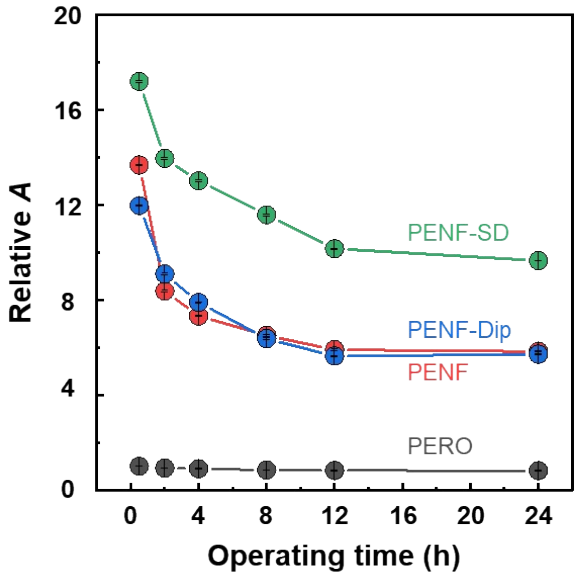

Fig. S7. Changes in the relative water permeance (*A*) of the membranes as a function of the operating time. Relative *A* was obtained by dividing the measured *A* by the initial *A* of the PERO membrane.

S8. Performance of reported positively charged and commercial NF membranes

Table S1. Water permeance (A), $MgCl_2$ rejection, and Li^+/Mg^{2+} selectivity ($S_{Li/Mg}$) measured under the corresponding simulative brine conditions ($MgCl_2$/LiCl mass ratio) of the membranes.

Reference	A (LMH bar^{-1})	$MgCl_2$ rejection (%)	$S_{Li/Mg}$	$MgCl_2$/LiCl mass ratio
Xu et al. (2019)[1]	5.0	94.8	20.0	20
Li et al. (2017)[2]	6.0	84.6	~12.7	24
Zhang et al. (2017)[3]	16.5	96.9	~16.4	21
Xu et al. (2020)[4]	11.2	~90	~16.1	20
Guo et al. (2020)[5]	4.2	~90	12.2	30
Liu et al. (2017)[6]	6.1	92.2	-	-
Wu et al. (2020)[7]	6.3	83.8	-	-
Zhu et al. (2016)[8]	3.9	94.9	-	-
Liu et al. (2012)[9]	8.5	90.5	-	-
Peydayesh et al. (2020)[10]	8.1	95.0	-	-
Shen et al. (2020)[11]	7.4	93.3	-	-
Huang et al. (2009)[12]	1.4	94.5	-	-
Huang et al. (2006)[13]	1.1	97.0	-	-
Yu et al. (2011)[14]	4.2	96.7	-	-
Yu et al. (2011)[14]	5.1	92.6	-	-
Yu et al. (2011)[14]	6.2	88.5	-	-
Sun et al. (2012)[15]	4.9	96.2	-	-
Wang et al. (2013)[16]	15.3	95.0	-	-
Ma et al. (2017)[17]	3.3	93.0	-	-
Li et al. (2011)[18]	6.0	93.2	-	-
Chen et al. (2017)[19]	0.3	92.6	-	-
Cui et al. (2015)[20]	7.0	93.2	-	-
Ji et al. (2015)[21]	3.4	96.0	-	-
NF90 (our study)	10.1 ± 1.5	99.0 ± 0.5	3.7	20
NF270 (our study)	16.3 ± 2.5	66.5 ± 2.0	3.9	20

References

1 P. Xu, W. Wang, X. Qian, H. Wang, C. Guo, N. Li, Z. Xu, K. Teng and Z. Wang, *Desalination*, 2019, **449**, 57.

2 W. Li, C. Shi, A. Zhou, X. He, Y. Sun and J. Zhang, *Sep. Purif. Technol.*, 2017, **186**, 233.

3 H. Z. Zhang, Z. L. Xu, H. Ding and Y. J. Tang, *Desalination*, 2017, **420**, 158.

4 P. Xu, J. Hong, X. M. Qian, Z. Z. Xu, H. Xia and Q. Q. Ni, *Desalination*, 2020, **488**, 114522.

5 C. Guo, N. Li, X. Qian, J. Shi, M. Jing, K. Teng and Z. Xu, *Sep. Purif. Technol.*, 2020, **230**, 115567.

6 C. Liu, W. Bi, D. Chen, S. Zhang, H. Mao, *Chin. J. Chem. Eng.,* 2017, **25**, 1685.

7 H. Wu, Y. Lin, W. Feng, T. Liu, L. Wang, H. Yao and X. Wang, *J. Membr. Sci.*, 2020, **603**, 117997.

8 J. Zhu, Q. Zhang, J. Zheng, S. Hou, H. Mao and S. Zhang, *J. Membr. Sci.*, 2016, **517**, 39.

9 M. Liu, Y. Zheng, S. Shuai, Q. Zhou, S. Yu and C. Gao, *Desalination*, 2012, **288**, 98.

10 M. Peydayesh, T. Mohammadi and S. K. Nikouzad, *J. Membr. Sci.*, 2020, **611**, 118205.

11 Q. Shen, S.-J. Xu, Z.-Q. Dong, H.-Z. Zhang, Z.-L. Xu and C. Y. Tang, *J. Membr. Sci.*, 2020, **610**, 118220.

12 R. Huang, G. Chen, M. Sun and C. Gao, *Desalination*, 2009, **239**, 38.

13 R. Huang, G. Chen, M. Sun, Y. Hu and C. Gao, *J. Membr. Sci.*, 2006, **286**, 237.

14 S. Yu, M. Ma, J. Liu, J. Tao, M. Liu and C. Gao, *J. Membr. Sci.*, 2011, **379**, 164.

15 S. P. Sun, T. A. Hatton, S. Y. Chan and T.-S. Chung, *J. Membr. Sci.*, 2012, **401**, 152.

16 T. Wang, Y. Yang, J. Zheng, Q. Zhang and S. Zhang, *J. Membr. Sci.*, 2013, **448**, 180.

17 X.-H. Ma, Z. Yang, Z.-K. Yao, Z.-L. Xu and C. Y. Tang, *J. Membr. Sci.*, 2017, **525**, 269.

18 X.-L. Li, L.-P. Zhu, Y.-Y. Xu, Z. Yi and B.-K. Zhu, *J. Membr. Sci.*, 2011, **374**, 33.

19 Y. Chen, F. Liu, Y. Wang, H. Lin and L. Han, *J. Membr. Sci.*, 2017, **537**, 407.

20 Y. Cui, Z.-K. Yao, K. Zheng, S.-Y. Du, B.-K. Zhu, L.-P. Zhu and C.-H. Du, *J. Membr. Sci.*, 2015, **492**, 187.

21 Y.-L. Ji, Q.-F. An, F.-Y. Zhao and C.-J. Gao, *Desalination*, 2015, **357**, 8.